Spectroscopy of lattice gauge theories from spectral densities

Niccolò Forzano

Dublin, 07/06/2024

Based on work [arXiv:2405.01388]
with E. Bennett, L. Del Debbio, R. Hill, D.K. Hong, H. Hsiao, J.W. Lee, C.-J.D. Lin, B. Lucini, A. Lupo, M. Piai, D. Vadacchino, F. Zierler

Overview

- Lattice setup.
- Benchmarks for our findings.
- **What** is spectral density?
- **How** do we study it?
- Numerical results.

Lattice setup

- We consider a $\mathrm{Sp}(4)$ gauge theory with $N_\mathrm{f} = 2$ (dynamical) fermions in the fundamental representation and $N_\mathrm{as} = 3$ in the 2-index antisymmetric one. → [Phys.Rev.D106 (2022) 1, 014501]

- We write the Euclidean action, discretised in four dimensions, as the sum of the gauge S_g and fermion S_f actions,

$$S \equiv S_g + S_f \,,$$

where

$$S_g \equiv \beta \sum_x \sum_{\mu<\nu} \left(1 - \frac{1}{2N} \mathrm{Re}\ \mathcal{P}_{\mu\nu}(x)\right),$$

$$S_f \equiv a^4 \sum_{j=1}^{N_\mathrm{f}} \sum_x \overline{Q}^j(x) D_m^{(\mathrm{f})} Q^j(x) + a^4 \sum_{j=1}^{N_\mathrm{as}} \sum_x \overline{\Psi}^j(x) D_m^{(\mathrm{as})} \Psi^j(x) \,,$$

- We perform simulation by using (rational) hybrid Monte-Carlo simulations (RHMC)

$$Z = \int \mathcal{D}U \mathcal{D}Q \mathcal{D}\bar{Q} \mathcal{D}\Psi \mathcal{D}\bar{\Psi}\, e^{-S[U,Q,\bar{Q},\Psi,\bar{\Psi}]}$$

LSDensities, new python library [https://github.com/LupoA/lsdensities]

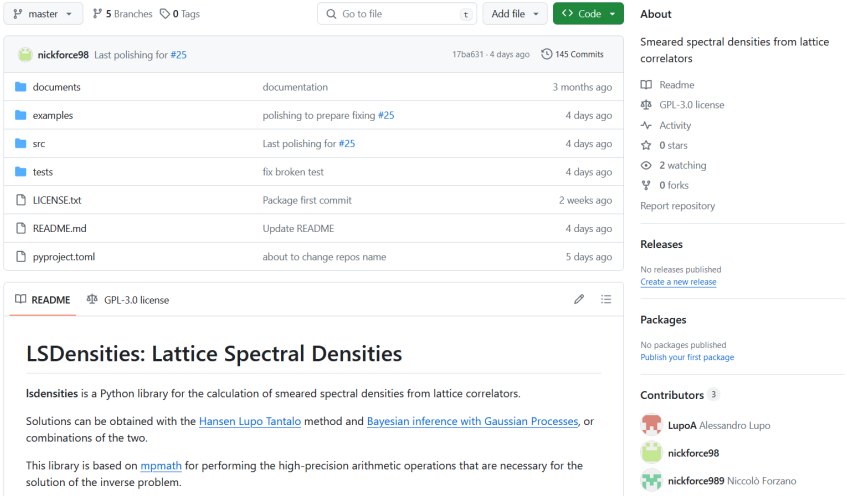

Benchmarks for our findings

- Comparisons with spectral density findings will be done using technologies already used in the literature:
  - Effective mass plateaus to isolate ground states

$$C(t) = \langle O(t)\bar{O}(0)\rangle \xrightarrow{t\to\infty} K \cdot e^{-M_0 t} \Rightarrow am_{\text{eff}} = -\ln\left[\frac{C(t+1)}{C(t)}\right]$$

  - Generalised Eigenvalue Problem (GEVP) to isolate excited states

$$C(t_2)v_n(t_2,t_1) = \lambda_n(t_2,t_1)C(t_1)v_n(t_2,t_1) \to \lambda_n(t_2,t_1)$$

where $C(t)$ is a matrix of correlation functions having the same spectrum.

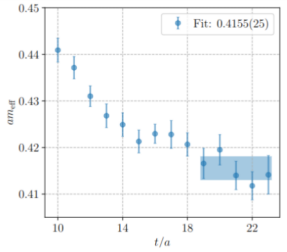

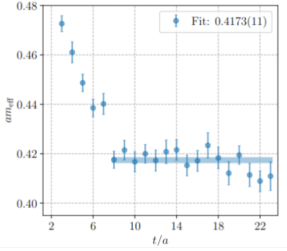

What is spectral density

- **What** is spectral density?

  → At positive Euclidean times $t \geq 0$ the previous correlator can be rewritten as

  $$C(t) = \int_0^\infty dE\, \rho_L(E) e^{-tE}$$

  and we defined

  $$\rho_L(E) = \langle 0|\mathcal{O}(0)\, \delta(E - H_L)\, \bar{\mathcal{O}}(0)|0\rangle_L$$

- Several applications:
  - Spectroscopy [arXiv:2212.08019].
    → Case study: Sp(4) theory with $N_f = 2$, $N_{as} = 3$ dynamical fermions.
  - Study of inclusive decay rates [arXiv:2111.12774].
  - Study of sphaleron rate (and maybe deconfinement?) [arXiv:2309.13327].

Spectral density extraction

To extract $\rho_L(E)$ from $C(t)$:

- Having a finite volume Hamiltonian H_L, we will have

$$\rho_L(E) = \sum_n w_n(L)\,\delta(E - E_n(L))$$

which is mostly lost in the continuum limit, where above the multi-particle threshold the spectral density becomes continuous.

→ We smear the spectral densities using a smearing kernel $\Delta_\sigma(E, \omega)$

$$\hat{\rho}_\sigma(\omega) = \int_0^\infty dE\,\Delta_\sigma(E, \omega)\rho_L(E)$$

(To be noted: correlator smearing ≠ spectral density smearing).

- We need to perform an inverse Laplace-transform which is **ill-posed**.

Ill-posed problem

- The problem is ill-posed. This can be seen by expanding

$$\bar{\Delta}_\sigma(E,\omega) = \sum_{t=0}^{t_{\max}} g_t(\omega) e^{-(t+1)E}$$

(therefore

$$\hat{\rho}(\omega) = \sum_{t=0}^{t_{\max}} g_t(\omega) C(t+1)$$

) and finding the coefficients $g_t(\omega)$ by minimizing

$$A[\vec{g}] = \int_0^\infty dE\, |\Delta_\sigma(E,\omega) - \bar{\Delta}_\sigma(E,\omega)|^2$$

- Therefore, if $C(t) = \bar{C}(t) + \delta(C(t))$ and the uncertainty on the spectral density $\delta(C(t)) \times g_t(E)$ will be uncontrolled.

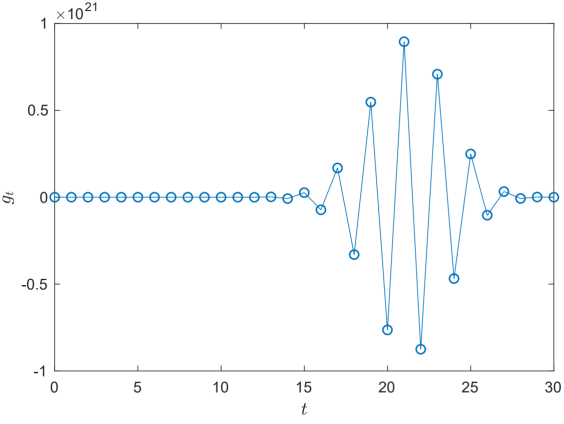

[arXiv:1903.06476]

Spectral density algorithm

We will reconstruct spectral densities using a modified Backus-Gilbert method: **HLT method** (Hansen-Tantalo-Lupo) [1].

To determine the vector of coefficients $\vec{g} = \vec{g}(E)$ for the spectral reconstruction, we minimize the functional

$$W[\vec{g}] = \frac{A[\vec{g}]}{A[0]} + \lambda \frac{B[\vec{g}]}{B_{\text{norm}}} \quad , \quad \lambda \in (0, \infty)$$

where $B_{\text{norm}} = C^2(1)/E^2$ (lattice spacing $a = 1$, for convenience)

$$A[\vec{g}] = \int_0^\infty dE\, e^{\alpha E}\, |\bar{\Delta}_\sigma(E, \omega) - \Delta_\sigma(E, \omega)|^2$$

$$B[\vec{g}] = \sum_{\tau,\, \tau'} g_\tau \, \text{Cov}_{\tau\tau'}[C]\, g_{\tau'}$$

For each energy we reconstruct the spectral density

$$\hat{\rho}(E) = \sum_t g_t(E)\, C(t)$$

Smearing kernels

In order to check the quality of reconstruction, we also check that at each energy the reconstruction of the kernels we use:

$$\bar{\Delta}_\sigma(E,\omega) = \sum_{t=0}^{t_{\max}} g_t(\omega) e^{-(t+1)E}$$

We use as target kernels:

- *Gaussian kernel*:

$$\bar{\Delta}^{(1)}_\sigma(E,\omega) = e^{-\frac{(E-\omega)^2}{2\sigma^2}} / Z(\omega)$$

with $Z(\omega) = \int_0^\infty dE\, e^{\frac{-(E-\omega)^2}{2\sigma^2}}$.

- *Cauchy kernel*:

$$\bar{\Delta}^{(2)}_\sigma(E,\omega) = \frac{\sigma}{\left[(E-\omega)^2 + \sigma^2\right]}$$

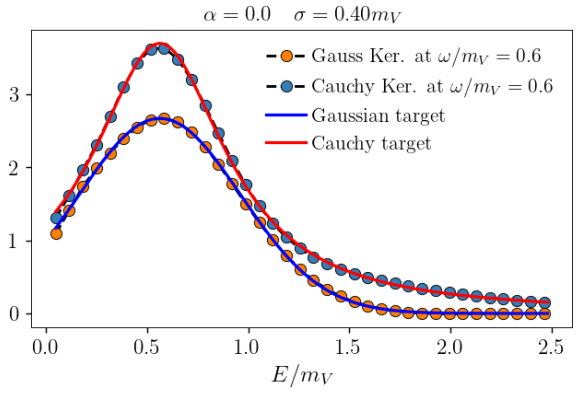

Spectral density reconstruction systematic errors

- Minimize

$$W[\vec{g}] = \frac{A[\vec{g}]}{A[0]} + \lambda \frac{B[\vec{g}]}{B_{\text{norm}}}$$

while varying α and λ.

- The first component of systematic error for each of these values $\hat{\rho}(E)$, will be estimated as

$$\sigma_{1,\,\text{sys}}(\hat{\rho}(E)) = |\hat{\rho}_{\lambda_*}(E) - \hat{\rho}_{\lambda_*/10}(E)|$$

where λ_* was found through the plateaus procedure described above.

- The second component of systematic error for each of the values $\hat{\rho}(E)$, will be estimated as

$$\sigma_{2,\,\text{sys}}(\hat{\rho}(E)) = |\hat{\rho}_{\lambda_*,\alpha_2}(E) - \hat{\rho}_{\lambda_*,\alpha_1}(E)|$$

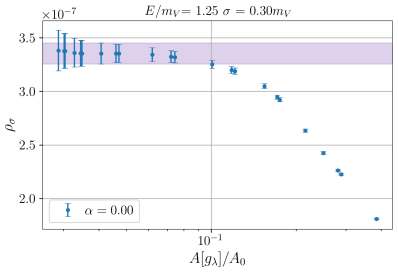

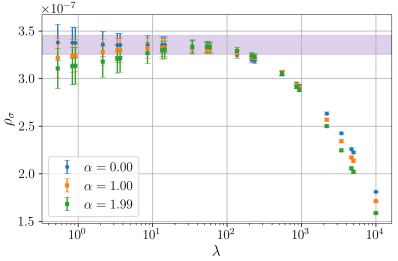

Spectral density fits

Given this procedure, we can perform fits of the spectral density, minimizing the functional [2]

$$\chi^2 = \sum_{E,\,E'} \left(f_\sigma^{(k)}(E) - \hat{\rho}_\sigma(E) \right) \mathrm{Cov}^{-1}_{E\,E'}[\hat{\rho}_\sigma] \left(f_\sigma^{(k)}(E') - \hat{\rho}_\sigma(E') \right)$$

where we fit the spectral densities as:

- Sum of Gaussians

$$f_\sigma^{(k)}(E) = \sum_{n=1}^{k} \mathcal{A}_n \, \Delta_\sigma^{(1)}(E - E_n)$$

- Sum of Cauchy functions

$$f_\sigma^{(k)}(E) = \sum_{n=1}^{k} \mathcal{A}_n \, \Delta_\sigma^{(2)}(E - E_n)$$

(remember that $\rho_L(E) = \sum_n w_n(L)\,\delta(E - E_n(L))$ and $\hat{\rho}_\sigma(\omega) = \int_0^\infty dE\, \Delta_\sigma(E, \omega)\rho(E)$)

Energy levels fitting: cross checks

- We perform several cross checks, for example we fit using both a Gaussian and Cauchy kernel

$$\sigma_{1,\,\mathrm{sys}}(aE_n) = |aE_{n,\,\mathrm{Gauss}} - aE_{n,\,\mathrm{Cauchy}}|$$

and we evaluate the difference between the same energy state, determined using the two kernels.

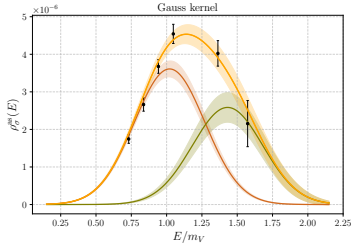

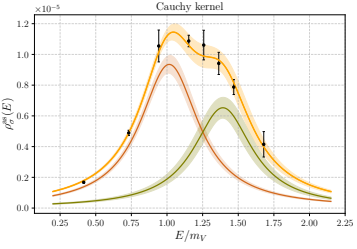

Improving the results: enlonging time extent

- We can increase values of N_t.

  → Increase basis to expand Kernel and spectral density, more accurate reconstruction.

$$\bar{\Delta}_\sigma(E.\omega) = \sum_{t=0}^{t_{\max}} g_t(\omega) e^{-(t+1)E}$$

(where $t_{\max} < T$).

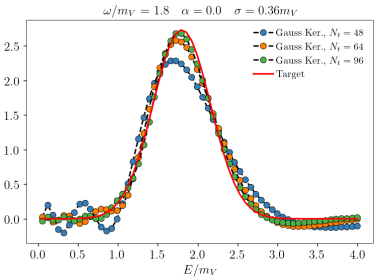

Numerical results: comparison with GEVPs

- We compare the GEVPs from several channels to check the excited states.

Channel	Interpolating operator
PS (F/AS)	$\bar{F}^i \gamma_5 F^j$
V (F/AS)	$\bar{F}^i \gamma_\mu F^j$
T (F/AS)	$\bar{F}^i \gamma_0 \gamma_\mu F^j$
AV (F/AS)	$\bar{F}^i \gamma_5 \gamma_\mu F^j$
AT (F/AS)	$\bar{F}^i \gamma_5 \gamma_0 \gamma_\mu F^j$
S (F/AS)	$\bar{F}^i F^j$

where i, j are flavour indices and $F = Q, \Psi$.

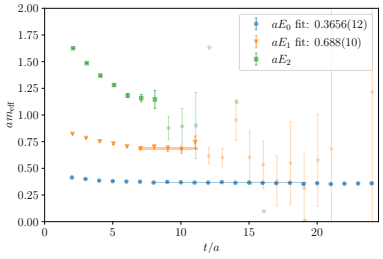

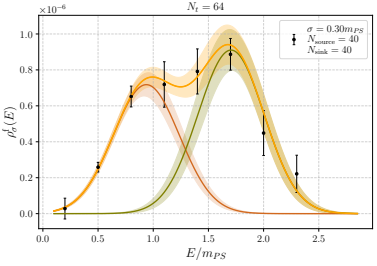

- They come out to be compatible within statistical uncertainty.

→ Example:

Channel	aE_0 (HLT)	aE_0 (GEVP)	aE_1 (HLT)	aE_1 (GEVP)
PS (f)	0.3652(11)	0.3656(12)	0.670(10)	0.688(10)

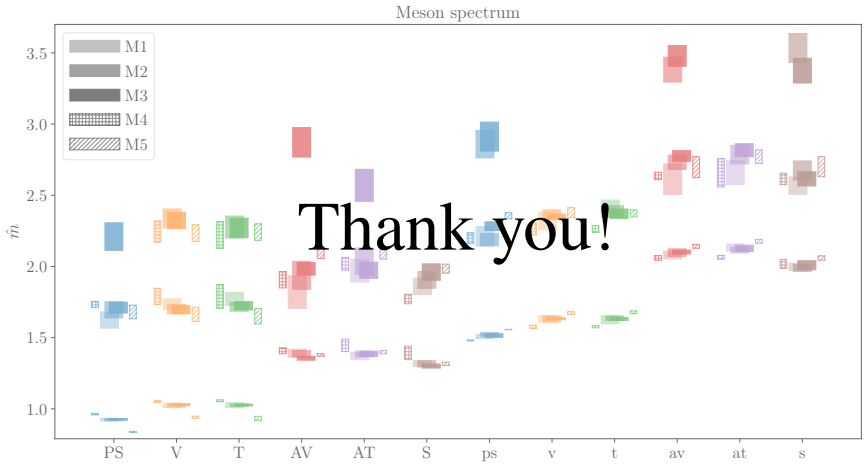
Meson spectrum
M1
M2
M3
M4
M5
3.5
3.0
2.5
2.0
1.5
1.0
$\hat{m}$
PS
V
T
AV
AT
S
ps
v
t
av
at
s

Thank you!

Bibliography

1. M. Hansen, A. Lupo and N. Tantalo, Phys. Rev. D **99** (2019) no.9, 094508 doi:10.1103/PhysRevD.99.094508 [arXiv:1903.06476 [hep-lat]].

2. A. Lupo, L. Del Debbio, M. Panero and N. Tantalo, PoS **LATTICE2022** (2023), 215 doi:10.22323/1.430.0215 [arXiv:2212.08019 [hep-lat]].

3. M. Albanese et al. [APE], Phys. Lett. B 192, 163-169 (1987) doi:10.1016/0370- 2693(87)91160-9

4. S. Gusken, Nucl. Phys. B Proc. Suppl. 17, 361-364 (1990) doi:10.1016/0920-5632(90)90273- W

Backup slides: $Sp(2N)$ Lie group

We denote as $Sp(2N)$ the subgroup of $SU(2N)$ preserving the norm induced by the antisymmetric matrix Ω,

$$\Omega = \begin{pmatrix} 0 & 1_N \\ -1_N & 0 \end{pmatrix} ,$$

where 1_N is the $N \times N$ identity matrix. This definition can be converted into a constraint on the group element U

$$U\Omega U^T = \Omega .$$

Due to unitarity, the previous condition can be also written as

$$U\Omega = \Omega U^* ,$$

which implies the following block structure

$$U = \begin{pmatrix} A & B \\ -B^* & A^* \end{pmatrix} ,$$

Backup slides: Wilson-Dirac operators on the lattice

The massive Wilson-Dirac operators are defined as

$$\begin{aligned} D_m^{(\mathrm{f})} Q^j(x) \quad &\equiv \quad (4/a + m_0^{\mathrm{f}}) Q^j(x) \\ &\quad -\frac{1}{2a} \sum_\mu \left\{ (1-\gamma_\mu) U_\mu^{(\mathrm{f})}(x) Q^j(x+\hat{\mu}) + (1+\gamma_\mu) U_\mu^{(\mathrm{f}),\,\dagger}(x-\hat{\mu}) Q^j(x-\hat{\mu}) \right\} , \end{aligned}$$

and

$$\begin{aligned} D_m^{(\mathrm{as})} \Psi^j(x) \quad &\equiv \quad (4/a + m_0^{\mathrm{as}}) \Psi^j(x) \\ &\quad -\frac{1}{2a} \sum_\mu \left\{ (1-\gamma_\mu) U_\mu^{(\mathrm{as})}(x) \Psi^j(x+\hat{\mu}) + (1+\gamma_\mu) U_\mu^{(\mathrm{as}),\,\dagger}(x-\hat{\mu}) \Psi^j(x-\hat{\mu}) \right\} , \end{aligned}$$

Backup slides: antisymmetric links definition

The link variables $U_\mu^{(\mathrm{as})}(x)$ are defined as follows:

$$U^{(\mathrm{as})}_{\mu,\,(ab)(cd)} = \left(e^{(ab)\,T} U_\mu^{(\mathrm{f})}\, e^{(cd)}\, U_\mu^{(\mathrm{f})\,\mathrm{T}}\right) ,$$

where $e^{(ab)}$ are the elements of an orthonormal basis in the $(N(2N-1)-1)$-dimensional space of $2N \times 2N$ antisymmetric and Ω-traceless matrices, and the multi-indices (ab) run over the values $1 \le a < b \le 2N$.
The entry ij of each element of the basis is defined as follows. For $b \neq N + a$,

$$e^{(ab)}_{ij} \equiv \frac{1}{\sqrt{2}} \left(\delta_{aj}\,\delta_{bi} - \delta_{ai}\,\delta_{bj}\right) ,$$

while for $b = N + a$ and $2 \le a \le N$,

$$e^{(ab)}_{i,i+N} = -e^{(ab)}_{i+N,i} \equiv \begin{cases} \frac{1}{\sqrt{2a(a-1)}} , & \text{for } i < a , \\ \frac{1-a}{\sqrt{2a(a-1)}} , & \text{for } i = a . \end{cases}$$

Backup slides: RHMC, rational hybrid Monte-Carlo

- The (R)HMC algorithms generate a Markov chain of gauge configurations distributed as required by the lattice action.
- Bosonic degrees of freedom ϕ and $\phi^\dagger$, known as pseudofermions, are introduced replacing a generic number n_f of fermions.
- Powers of the determinant of the hermitian Dirac operator, $Q_m^R = \gamma_5 D_m^R$, in representation R can then be expressed as

$$(\det D_m^R)^{n_f} = (\det Q_m^R)^{n_f} = \int \mathcal{D}\phi \mathcal{D}\phi^\dagger e^{-a^4 \sum_x \phi^\dagger(x)(Q_m^2)^{-n_f/2}\phi(x)} ,$$

- For odd values of n_f, the rational approximation is used to compute odd powers of the determinant above, resulting in the RHMC.

Backup slides: RHMC, rational hybrid Monte-Carlo (2)

- The fictitious hamiltonian is

$$H = \frac{1}{2} \sum_{x,\mu,a} \pi^a(x,\,\mu)\,\pi^a(x,\,\mu) + H_g + H_f\,,$$

- The molecular dynamics (MD) evolution in fictitious time τ is dictated by

$$\frac{\mathrm{d}U_\mu(x)}{\mathrm{d}\tau} = \pi(x,\,\mu)U_\mu(x)\,, \qquad \frac{\mathrm{d}\pi(x,\,\mu)}{\mathrm{d}\tau} = F(x,\mu)\,,$$

  where $F(x,\mu)$, known as the HMC force.

- Numerical integration of the MD equations thus leads to a new configuration of the gauge field, which is then accepted or rejected according to a Metropolis test.

Backup slides: formulas for spectral density reconstruction

- `A0_mp` and `A0E_mp`

$$A_0(\omega) \equiv A[0](\omega) = \int_{E_0}^{\infty} dE\, e^{\alpha E} \Delta_\sigma(E,\omega)^2 = \frac{e^{\frac{\alpha^2\sigma^2}{4}+\alpha\omega}\left(\mathrm{erf}\left(\frac{\alpha\sigma^2+2\omega-2e_0}{2\sigma}\right)+1\right)}{4\sqrt{\pi}\sigma}$$

- `ft_mp`

$$f_t(\omega) = \int_{E_0}^{\infty} dE\, \Delta_\sigma(E,\omega)\, b_T(t,E)\, e^{\alpha E}$$

$$= \frac{1}{2}\left\{ e^{\frac{1}{2}(\alpha+t-T)\left(\sigma^2(\alpha+t-T)+2\omega\right)}\left(\mathrm{erf}\left(\frac{\sigma^2(\alpha+t-T)+\omega-e_0}{\sqrt{2}\sigma}\right)+1\right)\right.$$

$$\left. + e^{\frac{1}{2}(\alpha-t)\left(\sigma^2(\alpha-t)+2\omega\right)}\mathrm{erfc}\left(\frac{\sigma^2(t-\alpha)-\omega+e_0}{\sqrt{2}\sigma}\right)\right\}$$

Backup slides: formulas for spectral density reconstruction (2)

- In the code, we express $f_t(\omega)$ by means of the following function called `generalised_ft`:

$$\tilde{f}_t(\omega) = e^{\frac{1}{2}(\alpha-t)\left(\sigma^2(\alpha-t)+2\omega\right)} \operatorname{erfc}\left(\frac{\sigma^2(t-\alpha)-\omega+e_0}{\sqrt{2}\sigma}\right) ,$$

  so that we can write $f_t(\omega) = \frac{\tilde{f}_t(\omega)+\tilde{f}_{T-t}(\omega)}{2}$

- `Smatrix_mp`

$$\mathtt{S}_{tr} = \frac{e^{E_0(\alpha-r-t-2)}}{t+r+2-\alpha} + \frac{e^{E_0(\alpha+r+t+2-2T)}}{2T-t-r-2-\alpha} + \frac{e^{E_0(\alpha+r-t-T)}}{T+t-r-\alpha} + \frac{e^{E_0(\alpha-r+t-T)}}{T-t+r-\alpha}$$

  We also have

$$\mathtt{B}_{tr} = \mathrm{Cov}_{tr} .$$

  $B_{\mathrm{norm}} = C(1)$ can be used to make $B[g]$ dimensionless.

- The minimisation then amounts to solve the following linear system

$$\vec{g} = \left(\mathtt{S} + \frac{\lambda A_0(\omega)}{(1-\lambda)(\omega)}\,\mathtt{B}\right)^{-1} \vec{\mathtt{f}} .$$

Backup slides: Numerical results: using Wuppertal and APE smearings

- We use APE [3] and Wuppertal smearing [4] to increase the overlap between the operators and the ground state

$$C(t) = \sum_n \frac{\langle 0|\mathcal{O}(0)|n\rangle\langle n|\bar{\mathcal{O}}(0)|0\rangle}{2E_n} e^{-tE}$$

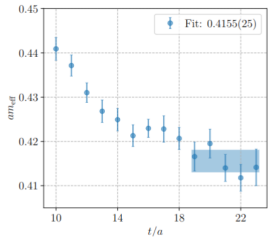

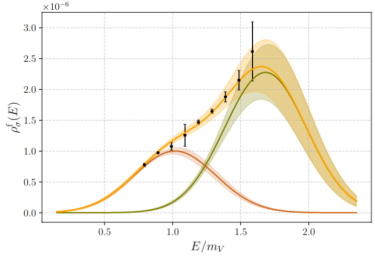

- Similarly we get

$$\hat{\rho}_\sigma(E) = \sum_n \frac{\langle 0|\mathcal{O}(0)|n\rangle\langle n|\bar{\mathcal{O}}(0)|0\rangle}{2E_n}$$

$$\times \Delta_\sigma(E - E_n(L))$$

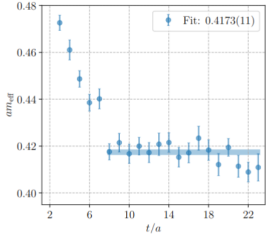

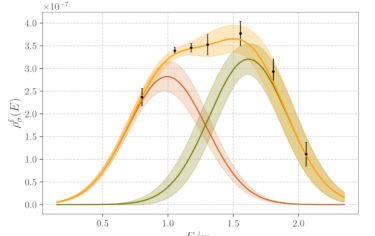

Backup slides: Wuppertal and APE smearings formulas

- Wuppertal smearing acts on fermion fields increasing the overlap of ground state.

$$q^{(n+1)}(x) = \frac{1}{1+2d\,\varepsilon}\left[q^{(n)}(x) + \varepsilon \sum_{\mu=\pm 1}^{\pm d} U_\mu(x) q^{(n)}(x+\hat{\mu})\right]$$

- APE smearing averages out UV fluctuations of the gauge fields.

$$U_\mu^{(n+1)}(x) = P\left\{(1-\alpha)U_\mu^{(n)}(x) + \frac{\alpha}{6} S_\mu^{(n)}(x)\right\}, \quad S_\mu(x) = \sum_{\pm\nu\neq\mu} U_\nu(x) U_\mu(x+\hat{\nu}) U_\nu^\dagger(x+\hat{\mu})$$

Backup slides: varying Wuppertal and APE smearings

Mean amplitudes ratios				
ϵ^{APE}	$\epsilon_{\mathrm{f}}^{\mathrm{Wuppertal}}$	N_{source}	N_{sink}	$\mathcal{A}_2/\mathcal{A}_1$
0.4	0.18	80	20	1.32(19)
0.4	0.18	80	40	1.15(11)
0.4	0.18	80	80	0.75(15)
0.4	0.18	40	80	1.24(18)
0.4	0.18	20	80	1.80(28)
0.4	0.24	90	30	1.01(20)
0.4	0.4	170	170	0.63(11)
0.4	0.05	20	20	2.28(27)
0.0	0.18	80	40	1.27(11)

Table: Amplitudes ratio between the two-gaussian fits, for different levels of sink and source Wuppertal smearing and APE smearing.

Backup slides: choosing smearing radius

- Choosing the correct smearing radius is delicate:
  - Too large choice make the fitting procedure difficult.
  - Too small one results in unreliable and even useless reconstruction.

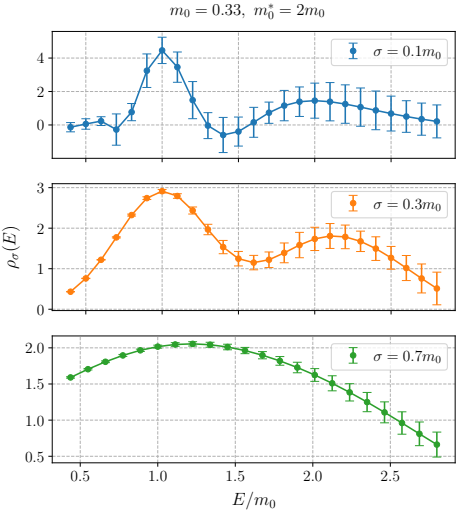

Backup slides: finiteness of information

- As the quantity of physical information in the input correlators is finite, the reconstruction will happen up to finite energies
  - The higher energies will become progressively less reliable.
  - Higher systematic effects entities.

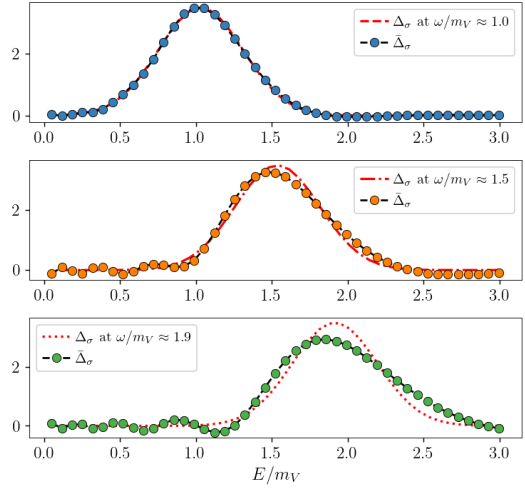

Backup slides: Numerical results: systematic errors evaluation

- The systematic errors due to excited states contaminations and change in kernel appears to be under controlled.

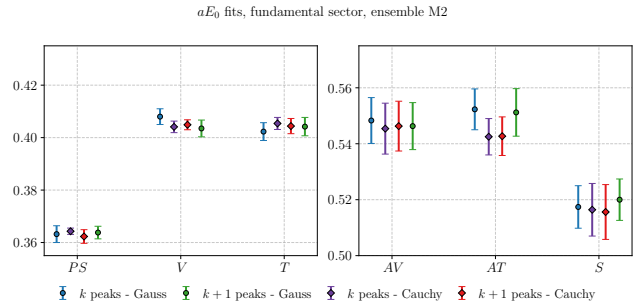

Backup slides: Improving the results: enlonging time extent

- We can increase values of N_t.

  → Increase basis to expand Kernel and spectral density, more accurate reconstruction.

$$\bar{\Delta}_\sigma(E.\omega) = \sum_{t=0}^{t_{\max}} g_t(\omega) e^{-(t+1)E}$$

(where $t_{\max} < T$).

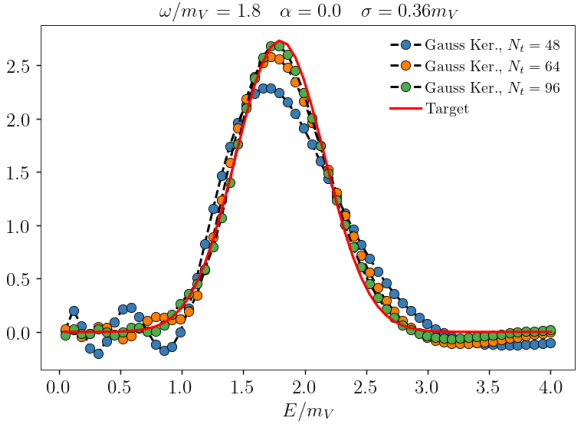

Backup slides: Improving the results: enlonging time extent (2)

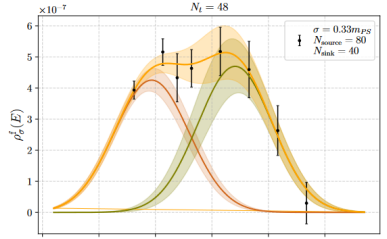

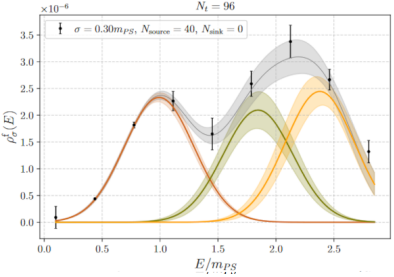

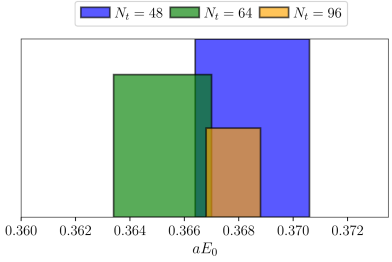

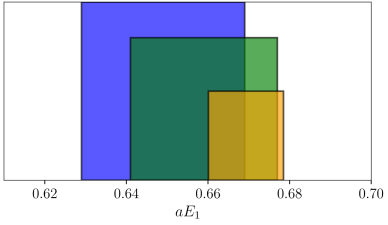

Backup slides: Outline

- We know how to reconstruct spectral densities → HLT algorithm.
- Systematics evaluation for $\rho(E)$ reconstruction can be done (α, λ variation).
- Fits of the finite volume spectral densities → Spectroscopy of gauge theories.
- Evaluation of systematics for energy levels aE_n → Different smearing kernels, $k/k+1$ peak fits.
- Spectroscopy results can be improved as we consider larger lattices.

Backup slide: Benchmarks for our findings

- Comparisons with spectral density findings will be done using technologies already used in the literature:
  - Effective mass plateaus to isolate ground states

$$C(t) = \langle O(t)\bar{O}(0)\rangle \xrightarrow{t\to\infty} K \cdot e^{-M_0 t} \Rightarrow am_{\text{eff}} = -\ln\left[\frac{C(t+1)}{C(t)}\right]$$

  - Generalised Eigenvalue Problem (GEVP) to isolate excited states

$$C(t_2)v_n(t_2,t_1) = \lambda_n(t_2,t_1)C(t_1)v_n(t_2,t_1) \to \lambda_n(t_2,t_1)$$

    where $C(t)$ is a matrix of correlation functions having the same spectrum.

- We will also use additional tools:
  - Wuppertal smearing, acting on fermion fields.
  - APE smearing, acting on gauge links.

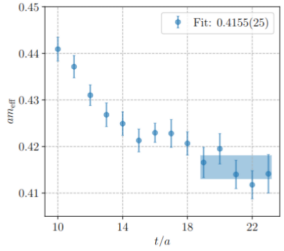

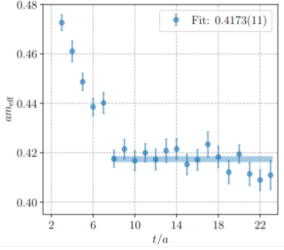

Backup slides: Ensembles

Label	β	am_0^f	am_0^{as}	$N_t \times N_s^3$
M1	6.5	-1.01	-0.71	48×20^3
M2	6.5	-1.01	-0.71	64×20^3
M3	6.5	-1.01	-0.71	96×20^3
M4	6.5	-1.01	-0.70	64×20^3
M5	6.5	-1.01	-0.72	64×32^3

Table: Ensembles generated for and analysed. The inverse coupling is denoted as β and the fundamental and antisymmetric bare fermion masses by am_0^f and am_0^{as}, respectively. The lattice volume is $N_t N_s^3 a^4$.

[Phys.Rev.D108 (2023) 9, 094508]

Backup slide: Energy levels fitting: cross checks

- We perform several cross checks, for example we fit using both a Gaussian and Cauchy kernel

$$\sigma_{1,\,\mathrm{sys}}(aE_n) = |aE_{n,\,\mathrm{Gauss}} - aE_{n,\,\mathrm{Cauchy}}|$$

  and we evaluate the difference between the same energy state, determined using the two kernels.

- Difference between the two and three Gaussian (or Cauchy) functions

$$\sigma_{2,\,\mathrm{sys}}(aE_n) = |aE_{n,\,k=3} - aE_{n,\,k=2}|$$